

Original Research

Biological Nitrogen Removal in a Flow-Separating Biochemical Reactor with Coral Sand

Xiangyu Long¹, Ran Tang^{1,2*}, Bo Zhan¹, Zhendong Fang¹,
Chaoxin Xie¹, Yongqin Li¹

¹Department of Military Installations, Army Logistics University of the People's Liberation Army,
University Town, Chongqing, China

²College of Chemistry and Chemical Engineering, Chongqing University of Science and Technology,
Chongqing, China

Received: 28 July 2018

Accepted: 27 October 2018

Abstract

In order to provide some support for economically and effectively resolving the problem of water pollution around the islands in the South China Sea, biological nitrogen removal (BNR) performance and biotechnological characterization of the FSBR filled with abandoned coral sand were investigated. The results showed that the TN removal efficiency of the FSBR with a good performance of simultaneous nitrification and denitrification (SND) was $74.68 \pm 6.49\%$ during the stable operation. The total biomass and removal efficiency of pollutants in the three reaction regions all decreased along the flow direction. Therefore, the first region was the key area for SND reaction and TN removal. In the first region, the nitrification process was the result of the combination of autotrophic nitrification and heterotrophic nitrification. Meanwhile, aerobic denitrification played a key role in the process of denitrification. In the region, the most denitrifying bacteria belonged to *Proteobacteria*, in which *unclassified_f_Comamonadace*, *Acidovorax* and *Dokdonella* were the major aerobic denitrifying bacteria.

Keywords: aerobic denitrification; biological nitrogen removal (BNR); coral sand; flow-separating biochemical reactor; simultaneous nitrification and denitrification (SND)

Introduction

With the development and construction of islands in the South China Sea, the problem of marine pollution from the discharge of domestic sewage becomes serious. The treatment of domestic sewage is an

important strategy to control the water environmental quality around the islands. Nitrogen is a key factor of waterbody eutrophication and an important object of domestic sewage treatment [1, 2]. At present, biological nitrogen removal (BNR) is an economical and effective way to remove nitrogen in domestic sewage [2]. In recent years, Simultaneous nitrification and denitrification (SND) has received wide attention [3-5]. Compared with the conventional anoxic/oxic (A/O) denitrification technology, SND has many

*e-mail: tangranhncq@126.com

advantages: (1) Saving occupation space and capital investment cost, (2) Reducing operating cost and energy consumption, and (3) Improving operational stability. Therefore, it is of great significance to offer an appropriate SND technology of domestic sewage treatment for the islands in the South China Sea.

Flow-separation biochemical reactor (FSBR) integrating the principles of biological contact oxidation and flow separation is an efficient wastewater treatment technology [6]. The technology has the characteristics of high efficiency and simple operation, without a secondary settling tank, mixed liquid recycle, sludge return and waste sludge discharge [7]. Therefore, the FSBR should be an appropriate technology for domestic sewage treatment of the islands. However, there were few reports on the SND performance of the FSBR.

In the process of SND, there were not only autotrophic nitrification and anoxic denitrification, but also heterotrophic nitrification and aerobic denitrification [8, 9]. Thereby, the BNR performance of FSBR should be closely related to microbial population. Furthermore, the microbial population of FSBR should be affected by different forms of microbial aggregate (including suspended solid, loosely attached biofilm and tightly attached biofilm) and pollutant concentrations (decreasing along the flow direction). In order to understand the performance and characteristics of BNR in the FSBR, it is necessary to investigate the microbial community characteristics in the different forms of microbial aggregate along the flow direction.

Coral sand is widespread in islands of the South China Sea, which has a rough surface and porous structure [10]. Therefore, coral sand should be suitable as a biofilm carrier. If utilizing abandoned coral sand as the filler of flow-separated ball, the construction cost of a sewage treatment system in the South China Sea could

be reduced substantially. In the study, abandoned coral sand was used as the filler of flow-separated ball in FSBR. In order to provide some support for economically and effectively resolving the problem of water pollution around the islands in the South China Sea, the BNR performance and biotechnological characterization of the FSBR were investigated. Firstly, nitrogen removal efficiency of the FSBR filled with abandoned coral sand was studied during the start-up and steady operation, after analyzing physicochemical properties of coral sand. Secondly, the changes of pollutant removal efficiency and microbial biomass along with the flow direction in the FSBR were analyzed to understand BNR performance. Finally, the microbial community characteristics of the different forms of microbial aggregate along the flow direction were investigated, and then the biotechnological characterization of BNR in the FSBR were discussed.

Material and Methods

Experimental Installation and Inflow Quality

A pilot-scale FSBR was used to treat domestic sewage in the West Campus of the Army Logistics University of PLA, China. The FSBR included a water-distribution area, a reaction area and an exhalant area (Fig. 1). The working volume of the reaction area was 0.576 m³. In addition, the reaction area was divided into three reaction regions by perforated plates, of which the perforated rate was 12.56%. In order to study pollutant removal efficiency along the flow direction, six sampling points were set at equal distance in the reaction area, where flow-separated balls made of polypropylene with a diameter of 10 cm

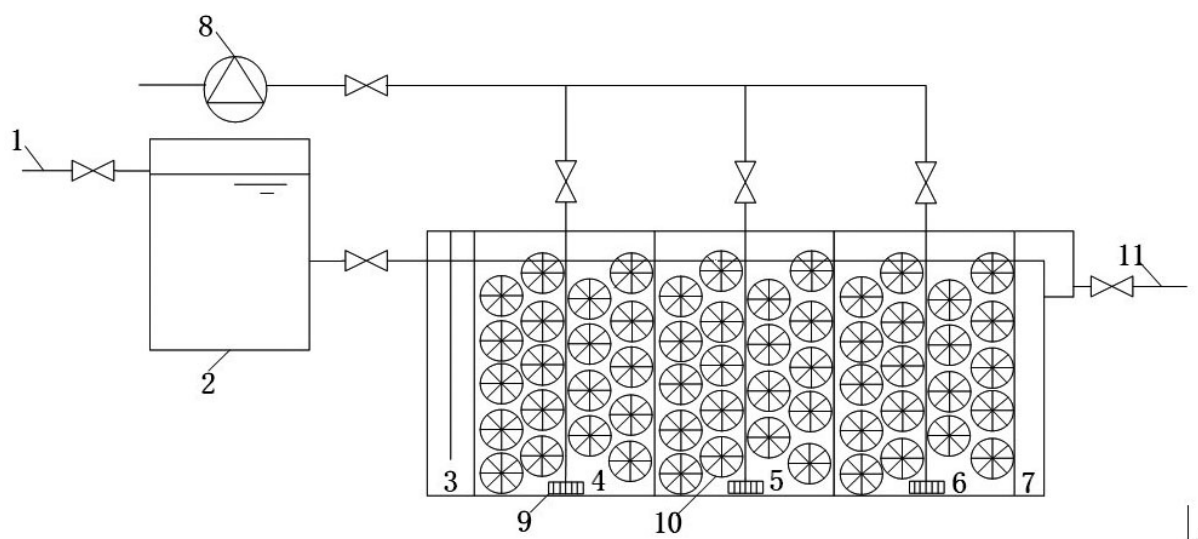


Fig. 1. Schematic diagram of flow-separating biochemical reactor: 1) Influx, 2) Head tank, 3) Water distribution area, 4) First reaction region, 5) Second reaction region, 6) Third reaction region, 7) Exhalant area, 8) Air pump, 9) Aerator, 10) Flow-separating ball, 11) Efflux.

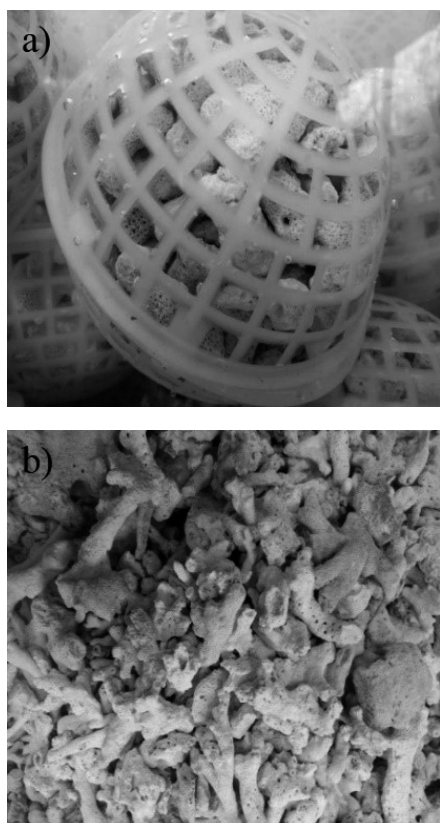


Fig. S1 a) Pictures of flow-separated ball ($\text{\O}10\text{mm}$) filled with coral sand; b) Pictures of Coral sand (1 mm~3 mm of effective particle size).

were packed (Fig. S1a), of which specific gravity was 0.91-0.93 g/cm^3 . In addition, the abandoned coral sands with an effective particle size of 1-3 cm were filled in flow-separated balls (Fig. S1b), which came from the process of infrastructure construction of an island of the Paracel Islands, China.

The domestic sewage was elevated into a head tank after filtration by wire screen (40 mesh). The quality of domestic sewage in the head tank is shown in Table 1. The average concentrations of COD, TN and $\text{NH}_4^+\text{-N}$ in inflow of the FSBR were 491 mg/L, 57.4 mg/L and 49.5 mg/L, respectively.

Startup and Operational Conditions

During start-up, the FSBR feed with domestic sewage was first run as a sequencing batch reactor for 6 days. Subsequently, the FSBR was operated as a continuous flow reactor. The continuous flow periods were divided into 4 stages, of which the main operating

parameters are shown in Table 2. In stage 1, when the FSBR was under startup conditions, the hydraulic retention time was gradually decreased and the ratio of air to water maintained a low value (15:1), which was beneficial to the growth of biofilms. From stage 2 to stage 4, the hydraulic retention time was controlled to 12 d or 16 d and the ratio of air to water was gradually increased in order to study the effect of the ratio of air to water on biological nitrogen removal in the FSBR. The water qualities of inflow and effluent were measured twice a day from day 1 to day 69 or once a day from day 70 to day 110, including the concentrations of COD, TN, $\text{NH}_4^+\text{-N}$, $\text{NO}_3^-\text{-N}$, $\text{NO}_2^-\text{-N}$ and DO, as well as pH value and water temperature.

Physicochemical Properties of Coral Sand

The microstructure and elemental composition of coral sand were measured by the scanning electron microscopy (SEM) equipped with energy disperse spectroscopy (EDS) (Quanta 250FEG, FEI, USA). The acceleration voltage of SEM (HV) was 15.00 KV, and the energy of EDS was 0.00 ~ 6.00 KeV. The phase composition of coral sand was measured by X-ray diffractometer (XRD) (D8 advance, Bruker, Germany).

Determining Microbial Biomass

Microbial aggregate in FSBR are classified into three forms, including suspended sludge, loosely attached biofilm and tightly attached biofilm. Suspended sludge concentration (in mg/L) was measured by the standard method [11]. The amounts of loosely attached biofilm and tightly attached biofilm were measured according to the procedures of Delatolla et al. [12]. Coral sand was rinsed 4 times with pure water and the rinsing fluids were collected, in which suspended solids were regarded as the loosely attached biofilm. Subsequently, the tightly attached biofilm sand was peeled off from the surface of coral sand with 0.1 N NaOH solution by water bath oscillation at 80°C. The amounts of loosely attached biofilm and tightly attached biofilm biomass were expressed as mg/g, respectively. They were also expressed as mg/L with the conversion coefficient, which was calculated as follows.

$$\text{Conversion coefficient} = \rho \times (1 - m) \times A \times 10^3 \quad (1)$$

Table 1. Inflow water quality of the FSBR.

Index	COD (mg/L)	TN (mg/L)	$\text{NH}_4^+\text{-N}$ (mg/L)	$\text{NO}_3^-\text{-N}$ (mg/L)	pH	C/N	T(°C)
Range value	125-1008	15.7-95.7	9.3-77.4	0.08-0.88	6.55-7.78	2.88-21.78	12.1-31.9
Average value	491	57.4	49.3	0.33	7.15	8.94	21.3

Table 2. Main operational parameters at different stages.

Stage	Runtime (d)	Duration (d)	Flowrate (L/h)	Hydraulic retention time (h)	Air water ratio
1	7-8	2	12	48	15, 1
	9-10	2	24	24	
	11-12	2	36	16	
	13-14	2	48	12	
2	15-32	18	48	12	15, 1
3	33-48	16	36	16	20, 1
4	49-110	62	36	16	25, 1

...where ρ is the density of coral sand (g/cm^3), which is $2.88 \text{ g}/\text{cm}^3$; m is the clearance ratio among flow-separated balls, which is around 0.38; and A is the filling rate of coral sand in flow-separated ball, which is about 0.30.

Calculating SND Ratio

The effect of microbial assimilation and cell lysis on the concentration of $\text{NH}_4^+\text{-N}$ was ignored in the process of calculating SND rate [5]. The calculation formula was as follows:

$$\text{SND}\% = \left(1 - \frac{\text{NO}_x^- \text{ produced}}{\text{NH}_4^+ \text{ removed}}\right) \times 100\% \quad (2)$$

...where $\text{NO}_x^- \text{ produced}$ is the difference between the sum of concentrations of $\text{NO}_2^- \text{-N}$ and $\text{NO}_3^- \text{-N}$ in effluent and inflow. $\text{NH}_4^+ \text{ removed}$ is the difference of concentrations of $\text{NH}_4^+\text{-N}$ in inflow and effluent.

Microbial Community Analysis

DNA Extraction

During stable operation (day 92), the samples of suspended sludge, loosely attached biofilm and tightly attached biofilm in the three reaction regions were collected, respectively. DNA was extracted by soil genomic DNA extraction kit (Tiangen Biochemical Technology Co., Ltd., Beijing, China). Then the DNA extract was stored at -20°C .

PCR Amplification and High-Throughput Sequencing

DNA samples were amplified by PCR using primer set 338F (5/-ACTCCTACGGG AGGCAGCAG-3/) and 806R (5/-GGACTACHVGGGTWTCTAAT-3/) for the V3-V4 region of 16S rRNA gene. The 20 μL mixture was used to perform PCR reaction, containing 4 μL 5_FastPfu Buffer, 2 μL dNTPs (2.5 mM), 0.8 μL each primer (5 μM), 0.4 μL of FastPfu polymerase, 0.2 μL BSA and 10 ng of template DNA. The PCR was performed in a GeneAmp_9700 (Applied

Biosystems, U.S.) with the following steps: 95°C for 3 min, followed by 27 cycles of denaturing at 94°C for 30 s, annealing at 55°C for 30 s, and extension at 72°C for 45 s, followed by a final extension at 72°C for 10 min. The PCR products were sequenced on an

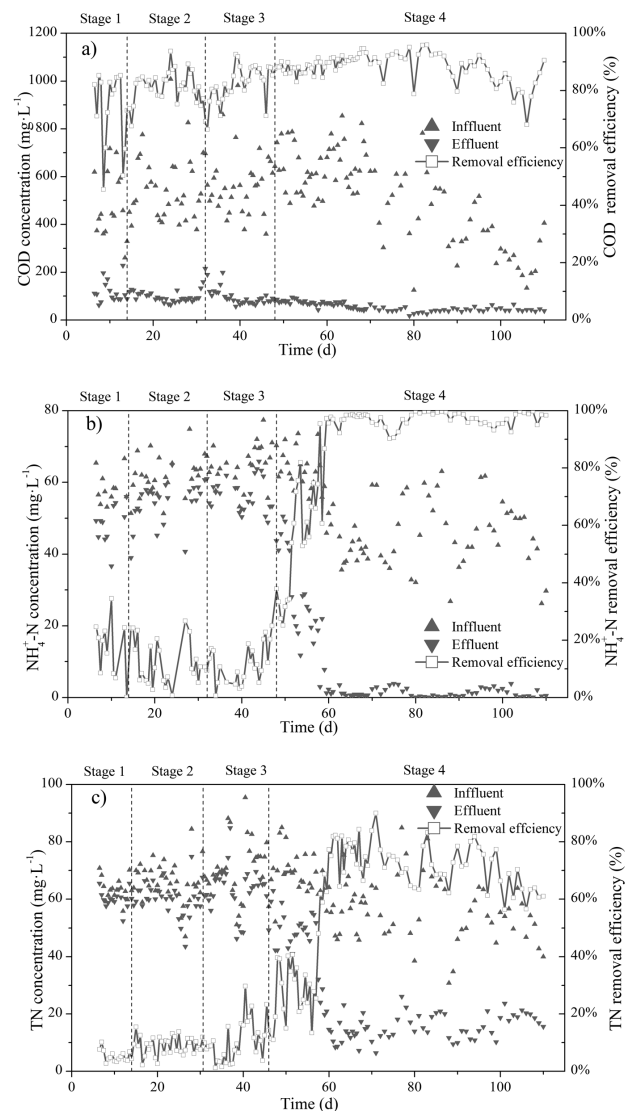


Fig. 2. Water quality changes of influent and effluent and removal efficiencies of pollutants: a) COD, b) $\text{NH}_4^+\text{-N}$, c) TN.

Illumina MiSeq PE300 platform according to the standard protocols. The raw sequences were deposited to the NCBI (serial number SPR123034).

Other Analytical Methods

The DO concentration and pH value in liquid phase was examined with a DO analyzer (Pro20, YSI, Ohio,

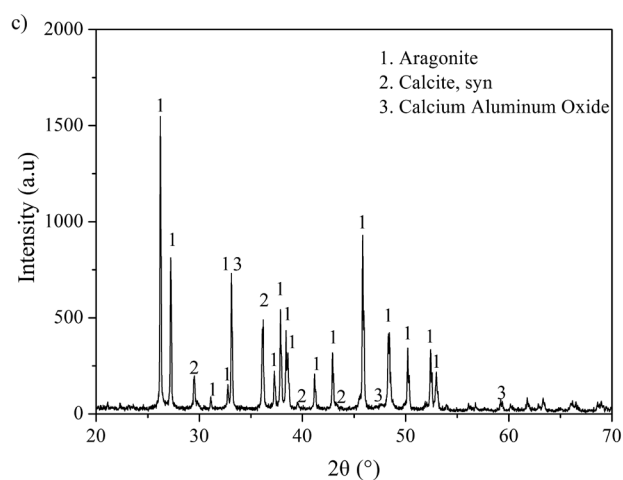
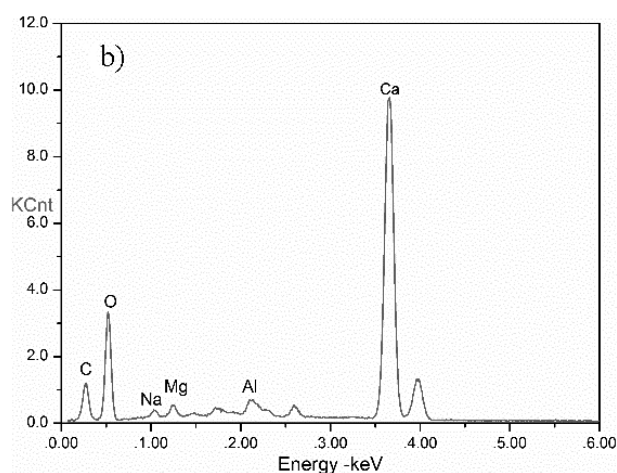
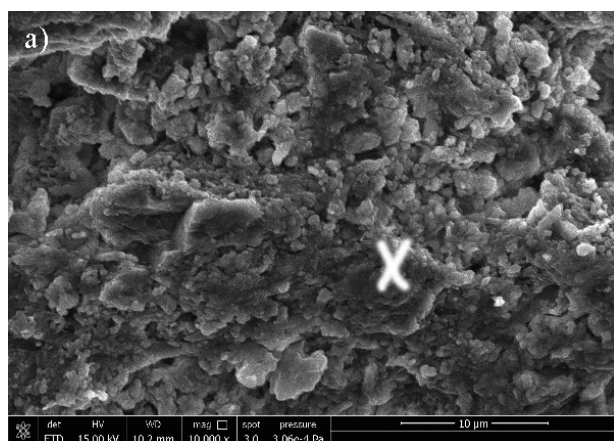


Fig. S2 a) SEM photograph of coral sand; b) EDS analysis of the point marked in the SEM image of coral sand; c) XRD spectra of coral sand.

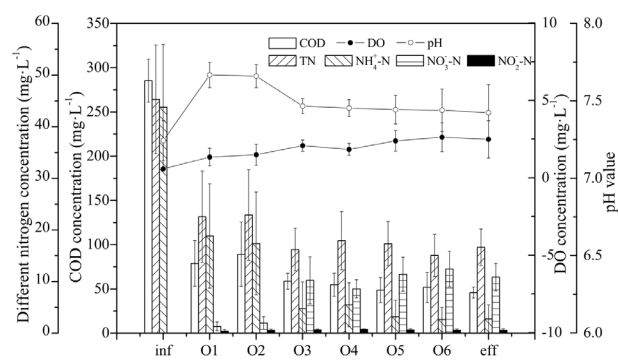


Fig. 3. Concentration of pollutants along flow direction.

USA) and a pH meter (PHBJ-260, Raytheon, Shanghai), respectively. The concentrations of COD, $\text{NH}_4^+\text{-N}$, $\text{NO}_2^-\text{-N}$, $\text{NO}_3^-\text{-N}$ and TN were measured according to the standard methods [11].

Results and Discussion

Physicochemical Properties of Coral Sand

As shown in the SEM image (Fig. S2a), the coral sand had a rough surface and porous structure, which should be beneficial to the attached growth of microorganisms. With the analysis of EDS (Fig. S2b), the main elements of coral sand were Ca, C and O. Furthermore, the mass percentages of Ca, C and O in coral sand were 22.02%~33.89%, 10.63%~10.97% and 53.00%~63.97%, respectively. As shown in the XRD spectra (Fig. S2c), the main phase composition of coral sand was metastable aragonite (CaCO_3), of which the other phase compositions included a small amount of stable calcite (CaCO_3) and tricalcium aluminate ($\text{Ca}_3\text{Al}_2\text{O}_6$). Both the calcite (CaCO_3) and tricalcium aluminate ($\text{Ca}_3\text{Al}_2\text{O}_6$) had good mechanical strengths, which might play key roles in the structural strength of coral sand. The results indicated that coral sand had good physicochemical properties as a biofilm carrier.

Removal Efficiency of Pollutants

As shown in Fig. 2, the removal efficiency of COD increased with the increase of air water ratio (from stage 2 to stage 4). After day 65, the removal efficiency of COD was stable ($88.16\% \pm 5.87\%$). In the initial phase of the start-up, the removal efficiencies of $\text{NH}_4^+\text{-N}$ and TN were low. From day 40 to day 60, the removal efficiencies increased rapidly. After day 60, the removal efficiencies were stable at the same time. The concentrations of $\text{NH}_4^+\text{-N}$ and TN in effluent were 1.25 ± 1.06 mg/L and 14.39 ± 4.37 mg/L, respectively. Meanwhile, the removal efficiencies of $\text{NH}_4^+\text{-N}$ and TN were $97.21 \pm 2.37\%$ and $74.68 \pm 6.49\%$, respectively. In addition, the SND rate was $80.50 \pm 9.38\%$. Importantly, there was a strong positive correlation between the removal efficiencies

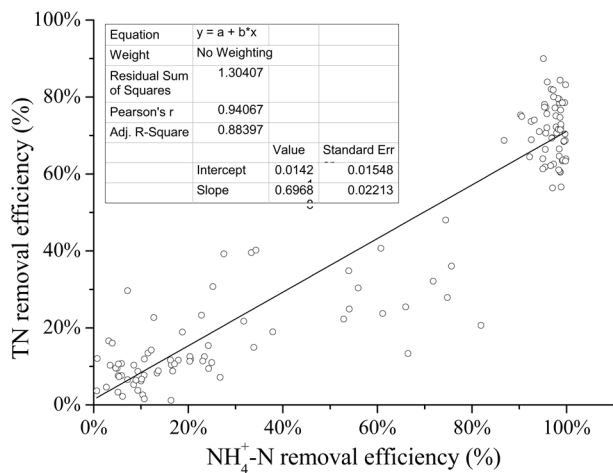


Fig. S3. Correlation between removal rates of $\text{NH}_4^+\text{-N}$ and TN.

of $\text{NH}_4^+\text{-N}$ and TN ($r_p = 0.941$, $p < 0.05$) (Fig. S3), indicating an obvious SND phenomenon. In stage 2, both the DO concentrations and pH values in effluent continued to decrease because of the lower air:water ratio (Fig. S4a). In stage 3 they continued to increase because of the higher air:water ratio. In stage 4, the DO concentrations in effluent were greater than 2 mg/L, and the pH values were maintained at between 7.25 and 7.75. After day 60, the higher DO concentration in effluent was corresponding to the higher pH value. Meanwhile, there was a strong positive correlation between the DO concentration and the pH value in effluent ($r_p = 0.645$, $p < 0.05$) (Fig. S4b). The results indicated that the FSBR had a good performance of SND, which could effectively compensate for the alkalinity consumption in nitrification process.

It was noteworthy that the phenomenon of alternating-accumulation of $\text{NO}_2^-\text{-N}$ and $\text{NO}_3^-\text{-N}$ occurred after day 40 (Fig. S5). From day 40 to day 59, the $\text{NO}_2^-\text{-N}$ concentration of effluent gradually increased. After day 60, the $\text{NO}_2^-\text{-N}$ concentration of effluent decreased rapidly, when the $\text{NO}_3^-\text{-N}$ concentration increased. This phenomenon suggested that nitrite-oxidizing bacteria (NOB) had been effectively enriched in the FSBR. The results indicated that ammonia-oxidizing bacteria (AOB) might be enriched earlier than NOB.

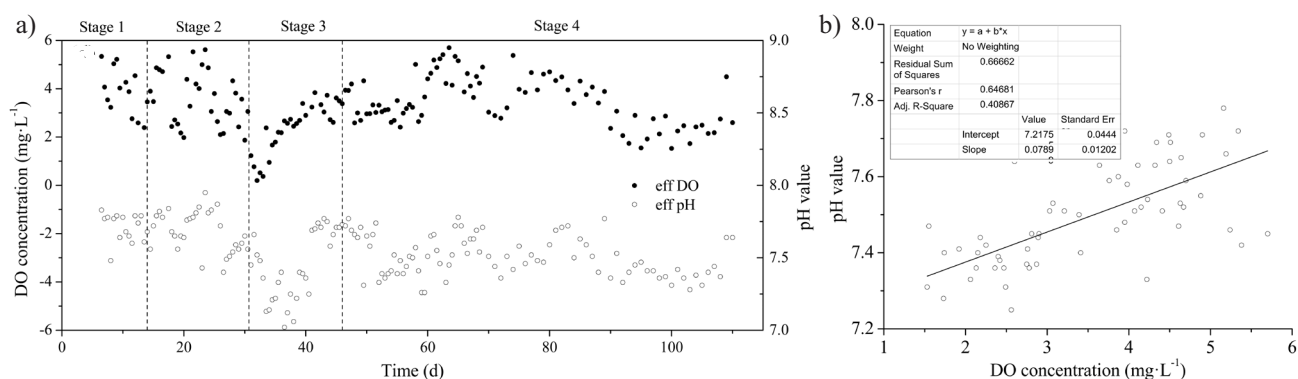


Fig. S4 a) DO concentration and pH value in effluent; b) Correlation between DO concentration and pH value in effluent.

Removal Efficiency of Pollutants Along Flow Direction

The reaction area of the FSBR was divided into three reaction regions. In addition, six sampling points were set at equal distance in the reaction area, which were marked as O1, O2, O3, O4, O5, and O6 along the flow direction, respectively. Namely, there were two sampling points in each reaction region. From day 70 to day 90, the removal efficiency of pollutants along the flow direction of the FSBR was investigated (Fig. 3 and Table 3). As shown in Fig. 3 and Table 3, the removal of pollutants mainly occurred in the first reaction region. In the first region, the DO concentration in liquid phase was 1.49 ± 0.07 mg/L. The removal efficiencies of COD, $\text{NH}_4^+\text{-N}$ and TN were $68.74 \pm 12.48\%$, $60.32 \pm 15.63\%$ and $49.50 \pm 9.29\%$, respectively. Simultaneously, the SND rate was $90.73 \pm 7.65\%$, suggesting that there was obvious SND in the first region. In the second region, the DO concentration in liquid phase was slightly increased (1.83 ± 0.05 mg/L). The $\text{NH}_4^+\text{-N}$ concentration in liquid phase was further decreased when the concentrations of COD and TN were slightly decreased. At the same time, the SND rate was $34.05 \pm 15.21\%$. Furthermore, the pH value of liquid phase in the second region was lower than that in the first region, suggesting that the nitrification in the second region consumed a lot of alkalinity. In the third region, the DO concentration of liquid phase was 2.62 ± 0.14 mg/L. In addition, the concentrations of COD, $\text{NH}_4^+\text{-N}$ and TN in liquid phase were slightly decreased, when $\text{NO}_3^-\text{-N}$ concentration was slightly increased and $\text{NO}_2^-\text{-N}$ concentration was reduced to near zero. The above results indicated that the first region was an important area for carbonation reaction and SND reaction.

Spatial Distribution Characteristics of Microbial Biomass

There were three forms of microbial aggregate in the FSBR, including suspended sludge, loosely attached biofilm and tightly attached biofilm. From day 70 to day 90, the spatial distribution characteristics of different forms of microbial aggregate in the FSBR

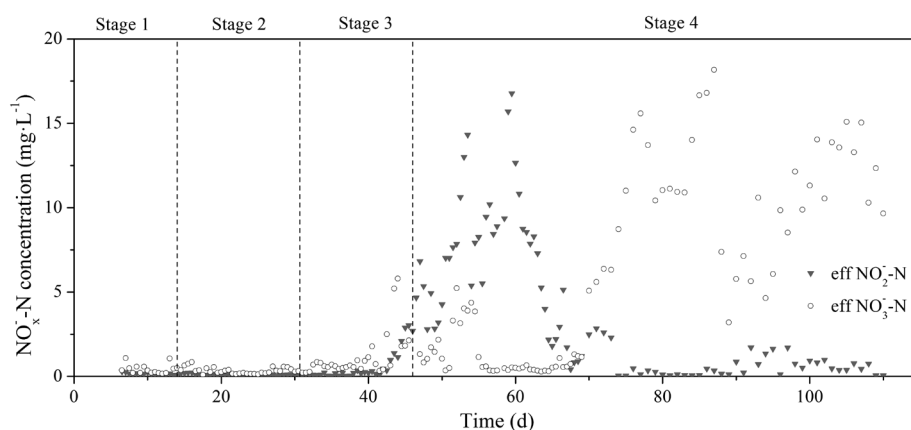


Fig. S5 NO_x-N concentration of effluent.

were investigated (Fig. 4). As shown in Fig. 4, the total biomass concentration and the biomass concentrations of three forms of microbial aggregate in the three reaction regions all decreased along the flow direction. The total biomass concentrations in the three regions along the flow direction were 7525.97±2084.55 mg/L, 3627.94±1173.07 mg/L and 2941.35±1032.59 mg/L, respectively. The total biomass concentration in the first region was 2.07 and 2.59 times of those in the second and third regions, respectively. The biomass concentrations of tightly attached biofilm in the three regions along the flow direction were 4731.29±1178.56 mg/L, 2309.20±751.23 mg/L and 1829.09± 494.04 mg/L, respectively, which were 62.87%, 63.65% and 62.19% of the corresponding total biomass concentrations. The results indicated that the tightly attached biofilm was an important microbial aggregate in the reactor. The biomass concentrations of loosely attached biofilm in the three regions along the flow direction were 1964.26±651.17mg/L, 1029±354.95mg/L and 1022.39±479.33mg/L, respectively. The concentrations of suspended sludge (SS) in the three regions along the flow direction were 830.43±252.82mg/L, 289.75±66.89mg/L and 89.88±59.22mg/L, respectively. The phenomenon of the rapid reduction of SS along the flow direction illustrated that the FSBR could save a secondary settling tank due to the effect of flow separation.

Microbial Community Structure

The microbial community structures of the three forms of microbial aggregate in the three reaction

regions were analyzed by high-throughput sequencing. From Table S1, the effective sequence numbers of community in the three forms of microbial aggregate of the three regions were 30064-44808, when the values of OUT were 973-1222 and the values of coverage were greater than 99%. Therefore, the results reflected the majority of microbial communities. In addition, the indexes of ACE, Chao, Shannon and Simpson illustrated that the richness and diversity of the microbial population of suspended sludge, loosely attached biofilm and tightly attached biofilm in the second and third regions were slightly more than those in the first region.

The percentages of community abundance on Genus level in the three reaction regions were shown in Fig. 5. In the first region, the main bacteria at

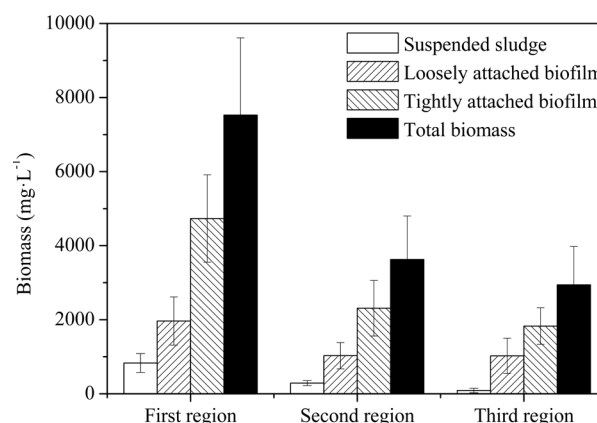


Fig. 4. Microbial biomass in the three regions of the FSBR.

Table 3. Removal efficiencies of pollutants in different reaction regions.

Index	COD	NH ₄ ⁺ -N	TN
First region	68.74±12.48%	60.32±15.63%	49.50±9.29%
Second region	12.09±9.96%	27.11±10.81%	10.96±7.03%
Third region	1.04±0.24%	6.51±3.96%	6.29±4.44%

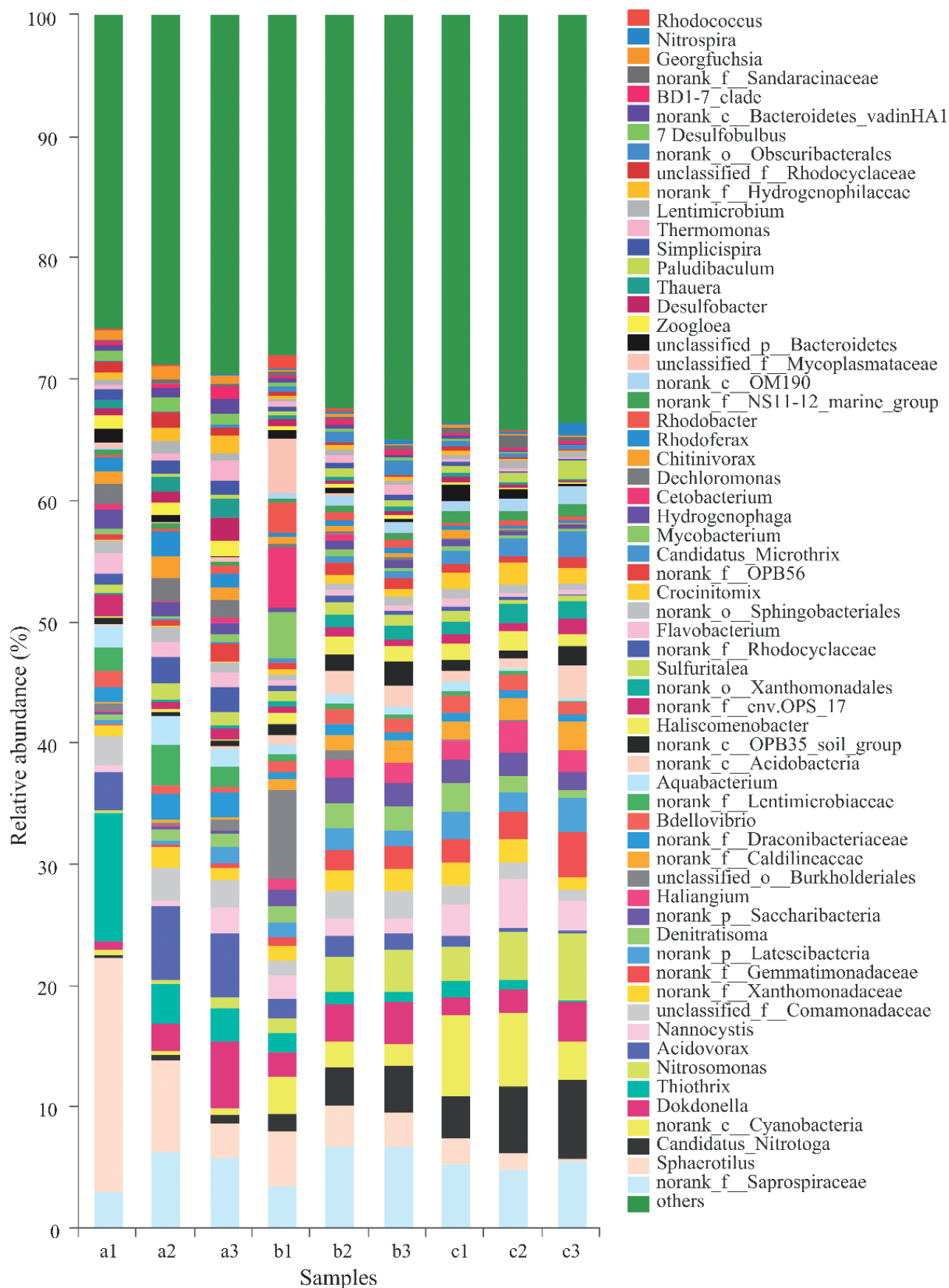


Fig. 5. Percentages of community abundance on genus level in different microbial aggregates of the three reaction regions (a, b and c represented the first, second and third reaction region, respectively; 1, 2 and 3 represented suspended sludge, loosely attached biofilm and tightly attached biofilm, respectively).

Table 4. Microbial population and their abundances on genus level participating in BNR in the FSBR.

Phylum	Class	Order	Family	Genus	Main function	a1	a2	a3	b1	b2	b3	c1	c2	c3
Proteobacteria	β -Proteobacteria	Burkholderiales	Comamonadaceae	<i>unclassified_f_Comamonadaceae</i>	Heterotrophic denitrification [4, 19]	2.72	3.24	2.72	1.42	2.58	2.73	1.66	1.71	1.13
				<i>Rhodoferax</i>	Heterotrophic denitrification [25]	1.18	2.03	1.08	0.35	0.41	0.38	0.35	0.18	0.12
				<i>Hydrogenophaga</i>	Heterotrophic denitrification [18]	1.59	1.12	0.85	0.38	0.68	0.66	0.56	0.32	0.27
				<i>Aquabacterium</i>	Aerobic denitrification [18]	1.80	2.33	1.50	0.86	0.75	0.67	0.77	0.28	0.17
				<i>Acidovorax</i>	Aerobic denitrification [4, 15]	3.11	5.94	5.02	1.52	1.71	1.36	0.94	0.37	0.22
				<i>Thauera</i>	Aerobic denitrification [24]	0.66	1.23	1.60	0.27	0.36	0.28	0.32	0.21	0.17
				<i>Zoogloea</i>	Heterotrophic denitrification [26]	1.17	1.02	1.25	0.38	0.36	0.37	0.31	0.18	0.15
				<i>norank_f_Rhodocyclaceae</i>	Aerobic denitrification [1]	0.91	1.28	0.72	0.28	-	0.26	0.26	0.10	0.06
				<i>Denitratisona</i>	Aerobic denitrification [18]	0.46	0.88	1.09	1.40	2.12	1.96	2.37	1.29	0.73
				<i>Dechloromonas</i>	Solid phase denitrification [27]	1.67	1.85	1.46	0.33	0.29	0.25	0.15	0.01	0.04
				<i>norank_f_Hydrogenophilaceae</i>	Heterotrophic denitrification [21]	0.55	1.12	1.48	0.24	0.29	0.27	0.33	0.16	0.11
				Cyanobacteria	γ -Proteobacteria	Nitrosomonadales	<i>Nitrosomonadaceae</i>	Ammonoxidation [21]	0.19	0.44	0.89	1.28	2.92	3.51
<i>Candidatus_Nitrotoga</i>	Nitrite oxidation [22]	0.16	0.67				0.50	1.41	3.09	3.88	3.45	5.56	6.51	
<i>Dokdonella</i>	Heterotrophic nitrification-Aerobic denitrification [16, 17]	0.71	2.23				5.57	2.00	3.05	3.57	1.54	1.96	3.29	
<i>Thiothrix</i>	Autotrophic denitrification [14]	10.55	3.20				2.72	1.55	1.00	0.73	1.25	0.73	0.15	
<i>Nannocystis</i>	Nitrite oxidation [16, 17]	0.47	0.39				2.14	1.99	1.47	1.18	2.59	4.00	2.44	
<i>Haliangium</i>	Heterotrophic denitrification [21]	-	-				-	0.94	1.43	1.68	1.63	2.61	1.76	
<i>norank_c_Cyanobacteria</i>	Biological nitrogen fixation [20]	0.48	0.35				0.55	3.11	2.17	1.74	6.66	6.08	3.14	
<i>norank_f_Caldilineaceae</i>	Heterotrophic denitrification [8]	0.05	0.20				0.24	0.88	1.28	1.72	1.49	1.80	2.33	
<i>norank_f_Gemmatimonadaceae</i>	Heterotrophic denitrification [28]	2.72	3.24				2.72	1.42	2.58	2.73	1.66	1.71	1.13	
<i>norank_c_Nitrospira</i>	Nitrite oxidation [21]	-	-				-	0.06	0.27	0.41	0.14	0.30	1.09	

a, b and c represented the first, second and third reaction region, respectively. 1, 2 and 3 represented suspended sludge, loosely attached biofilm and tightly attached biofilm, respectively.

genus level in suspended sludge included *Sphaerotilus* (19.26%), *Thiothrix* (10.55%), *Acidovorax* (3.11%), *norank_f_Saprospiraceae* (3.09%) and *unclassified_f_Comamonadaceae* (2.12%). The main bacteria at genus level in loosely attached biofilm included *Sphaerotilus* (7.59%), *norank_f_Saprospiraceae* (6.26%), *Acidovorax* (5.94%), *norank_f_Lentimicrobiaceae* (3.38%), *unclassified_f_Comamonadaceae* (3.24%), *Thiothrix* (3.20%), *Aquabacterium* (2.33%) and *Dokdonella* (2.23%). The main bacteria at genus level in tightly attached biofilm were *norank_f_Saprospiraceae* (5.85%), *Dokdonella* (5.57%), *Acidovorax* (5.02%), *Sphaerotilus* (2.84%), *unclassified_f_Comamonadaceae* (2.72%) and *Thiothrix* (2.72%). In these bacteria, *Sphaerotilus*, *Thiothrix*, *Acidovorax*, *unclassified_f_Comamonadaceae*, *Aquabacterium* and *Dokdonella* all belonged to *Proteobacteria*. Both *Sphaerotilus* and *Saprospiraceae* were common microorganisms with organic substance degradation [13]. In the first region, the abundance of *Sphaerotilus* in suspended sludge was more than those in loosely attached biofilm and tightly attached biofilm. However, the abundance of *norank_f_Saprospiraceae* in suspended sludge was lower than those in loosely attached biofilm and tightly attached biofilm. *Thiothrix* was an autotrophic denitrifying bacterium [14], which was abundant in suspended sludge of the first region. In the first region, the order of the *Thiothrix* abundance in the three forms of microbial aggregate was as follows: suspended sludge > loosely attached biofilm > tightly attached biofilm. In addition, *Acidovorax* [4, 15], *Dokdonella* [16, 17], *Aquabacterium* [18] and *unclassified_f_Comamonadaceae* [19] are aerobic denitrifying bacteria. In the first region, their abundances in tightly attached biofilm and loosely attached biofilm were obviously more than that in suspended sludge. The results indicated that there were significant differences of the abundances of bacteria with organic substance degradation and/or BNR among in the three forms of microbial aggregate in the first region.

In the second and third regions, the microbial community structures of loosely attached biofilm and tightly attached biofilm were similar, which were different from that of suspended sludge. In the three forms of microbial aggregate in the different regions, the abundance variation along the flow direction of *Sphaerotilus* was consistent with the change of COD removal efficiency. The abundance variation along the flow direction of *Norank_f_Saprospiraceae* in the three forms of microbial aggregate was not obvious because *Saprospiraceae* could not only utilize organic substance in inflow, but also metabolize cell fragments [13]. (By the way, *Cyanobacteria* was a photosynthetic bacteria with nitrogen fixation performance [20]). In the third region, there was a great deal of *norank_c_Cyanobacteria* in the three forms of microbial aggregate, suggesting that water quality had been significantly improved.

Biotechnological Characterization of SND in FSBR

In the study, domestic sewage was used as the influent. Therefore, there was a greater diversity of microbial communities taking part in BNR in the FSBR (Table 4). As shown in Table 4, the main aerobic AOB in FSBR was *Nitrosomonas* [21], and the main NOB included *Candidatus nitrotoga* [22], *Nitrospira* [21] and *Nannocystis* [16, 17]. In the three regions, the abundance of *Nitrosomonas*, *Candidatus nitrotoga* and *Nitrospira* in the three forms of microbial aggregate all increased along the flow direction. In the first region, the abundance of *Nitrosomonas* in suspended sludge, loosely attached biofilm and tightly attached biofilm were 0.19%, 0.44% and 0.89%, respectively, suggesting that aerobic ammonia oxidation mostly occurred in tightly attached biofilm. Moreover, *Nannocystis* was an important NOB in the tightly attached biofilm of the first region, of which the abundance (2.14%) was 4.19 times of that of *Candidatus nitrotoga* and far more than that of *Nitrospira*. Compared with the above nitrifying bacteria, denitrifying bacteria had higher abundance and population diversity in the first region. These denitrifying bacteria mainly belonged to six families of *Proteobacteria*, such as *Comamonadaceae*, *Rhodocyclaceae*, *Hydrogenophilaceae*, *Xanthomonadaceae*, *Thiotrichaceae* and *Haliangiaceae*. In the first region, the sum of their abundances in suspended sludge, loosely attached biofilm and tightly attached biofilm were 27.08%, 27.47% and 27.06%, respectively, which were 2.27, 1.83 and 1.78 times those in the second region and were 2.18, 2.72 and 3.23 times those in the third region. In addition, the total biomass in the first region was 2.07 and 2.56 times of that in the second and third regions, in which the amount of tightly attached biofilm was 62.87% (Fig. 4). The above results indicated that the tightly attached biofilm in the first region was a key microbial aggregate of SND reaction.

According to the types of electron donors, denitrification can be divided into autotrophic denitrification (AD) and heterotrophic denitrification (HD). *Thiothrix* is sulfide-autotrophic denitrifying bacteria, which utilizes sulfide or sulfur-containing organics as electron donor and nitrite or nitrate as electron acceptor, as well as carbonates (CO_3^{2-} and HCO_3^-) as carbon source [14]. In the FSBR, the coral sand was the filler of flow-separated balls, of which the main component is metastable aragonite (CaCO_3) (Fig. S2c). The coral sand could slowly and persistently release HCO_3^- to liquid phase [10], providing a carbon source for metabolism of *Thiothrix*. Meanwhile, domestic sewage contained some sulfide and organic sulfur compounds [23] that could offer an electron donor for metabolism of *Thiothrix*. Therefore, there were a large number of *Thiothrix* in the suspended sludge, loosely attached biofilm and tightly attached biofilm of the first region, of which their abundances were 10.55%, 3.20% and 2.72%, respectively. Notably,

Thiothrix was abundant in the suspended sludge of the first region. In addition, the abundances of *Thiothrix* in the three forms of microbial aggregate all decreased along the flow direction. In the FSBR, *Proteobacteria* participating in HD included *Comamonadaceae* (such as *unclassified_f_Comamonadaceae*, *Rhodoferrax*, *Hydrogenophaga*, *Aquabacterium* and *Acidovorax*), *Rhodocyclaceae* (such as *Thauera*, *Zoogloea*, *Norank_f_Rhodocyclaceae*, *Denitratisoma*, *Dechloromonas*) and *Hydrogenophilaceae* (such as *norank_f_Hydrogenophilaceae*) in β -*Proteobacteria*, *Xanthomonadaceae* (such as *Dokdonella*) in γ -*Proteobacteria*, and *Haliangiaceae* (such as *Haliangium*) in δ -*Proteobacteria*. In the first region, *unclassified_f_Comamonadaceae*, *Acidovorax* and *Dokdonella* were the major HD bacteria. The abundances of *unclassified_f_Comamonadaceae* in suspended sludge, loosely attached biofilm and tightly attached biofilm were 2.72%, 3.24% and 2.72%, respectively. The abundances of *Acidovorax* in the above three forms of microbial aggregate were 3.11%, 5.94% and 5.02%, respectively. The abundance of *Dokdonella* in the above three forms of microbial aggregate were 0.71%, 2.23% and 5.57%, respectively. It has been reported that *unclassified_f_Comamonadaceae* [4, 19, 15], *Aquabacterium* [18], *Acidovorax* [4, 15], *Thauera* [24], *norank_f_Rhodocyclaceae* [1], *Denitratisoma* [18] and *Dokdonella* [16, 17] were aerobic denitrifying bacteria. In the first region, their total abundances in suspended sludge, loosely attached biofilm and tightly attached biofilm were 10.37%, 17.13% and 18.22%, respectively. Furthermore, the abundances of *Rhodoferrax*, *Hydrogenophaga*, *Zoogloea*, *norank_f_Hydrogenophilaceae* and *Dechloromonas* in the three forms of microbial aggregate also decreased along the flow direction, which was similar to the variations of the abundances of the above seven aerobic denitrifying bacteria, suggesting that they all might be aerobic denitrifying bacteria. These results indicated that aerobic denitrification played a key role in denitrification.

The first region removing 49.50±9.29% of TN was the key area for TN removal. However, the amounts of autotrophic AOB and NOB all were far lower than those of sulfide-autotrophic denitrifying bacteria and aerobic denitrifying bacteria in the three forms of microbial aggregate of the first region. Furthermore, the abundances of AOB and NOB in the three forms of microbial aggregate all increased along the flow direction. It had been reported that most aerobic denitrifying bacteria had the function of heterotrophic nitrification [2]. Thereby, heterotrophic nitrification-aerobic denitrifying bacteria played an important role in SND [2, 9]. In previous studies, little attention has been paid to heterotrophic nitrification-aerobic denitrifying bacteria in *Proteobacteria*. Only *Dokdonella* was known as an heterotrophic nitrification-aerobic denitrification bacteria. In the study, *Dokdonella* was enriched in the tightly attached biofilm of the first region, of which the abundance was 5.57%. Although autotrophic

nitrifying bacteria had strong nitrification ability [21], heterotrophic nitrification-aerobic denitrifying bacteria were more suitable for high organic loading environmental conditions [2]. Thereby, the nitrification process in the first region should be the result of a combination of autotrophic nitrification and heterotrophic nitrification.

Conclusions

Coral sand had rough surface and porous structure, which was suitable as a biofilm carrier. The FSBR filled with abandoned coral sand had a good performance of SND, in which there was a strong positive correlation between the removal efficiencies of $\text{NH}_4^+\text{-N}$ and TN. In the period of stable operation, the TN removal efficiency of the FSBR was 74.68±6.49%, when the ratio of air to water was 25:1 and the DO concentrations in effluent were greater than 2 mg/L. Meanwhile, there was a strong positive correlation between the DO concentration and the pH value in effluent, indicating that the SND in FSBR could effectively compensate for alkalinity consumption in the nitrification process. In addition, the tightly attached biofilm was an important microbial aggregate, of which the amount was 62.19-63.65% of the total biomass. The total biomass and removal efficiencies of pollutants in the three reaction regions all decreased along the flow direction. Thereby, the first region was the key area for SND reaction and TN removal. In the first region, the nitrification process was the result of the combination of autotrophic nitrification and heterotrophic nitrification. Meanwhile, aerobic denitrification played a key role in the process of denitrification. In the region, the most denitrifying bacteria belonged to *Proteobacteria*, in which *unclassified_f_Comamonadaceae*, *Acidovorax* and *Dokdonella* were the major aerobic denitrifying bacteria.

Acknowledgements

This work was supported by the National Natural Science Foundation of China [grant No. 21577174] and the Chongqing Basic Science and Advanced Technology Research [grant Nos. CSTC2015jcyjB0390, CSTC2014jcyjA20004, and CSTC2015jcyjA20012].

Conflicts of Interest

The authors declare no conflict of interest.

References

1. KIM E., SHIN S.G., MAH J., TONGCO J.V., HWANG S. Use of food waste-recycling wastewater as alternative

- carbon source for denitrification process: A full-scale study. *Bioresource Technology*. **245**, 1016, **2017**.
2. WANG J., GONG B., HUANG W., WANG Y., ZHOU J. Bacterial community structure in simultaneous nitrification, denitrification and organic matter removal process treating saline mustard tuber wastewater as revealed by 16S rRNA sequencing. *Bioresource Technology*. **228**, 31, **2017**.
 3. ZHAO J., FENG L., YANG G., DAI J., MU J. Development of simultaneous nitrification-denitrification (SND) and organics removal in biofilm reactors with partially coupled a novel biodegradable carrier for nitrogen-rich water purification. *Bioresource Technology*. **243**, 800, **2017**.
 4. RUAN Y.J., DENG Y.L., GUO X.S., TIMMONS M.B., LU H.F., HAN Z.Y., YE Z.Y., SHI M.M., ZHU S.M. Simultaneous ammonia and nitrate removal in an airlift reactor using poly (butylene succinate) as carbon source and biofilm carrier. *Bioresource Technology*. **216**, 1004, **2016**.
 5. THIRD K.A., BURNETT N., CORD-RUWISCH R. Simultaneous nitrification and denitrification using stored substrate (PHB) as the electron donor in an SBR. *Biotechnology & Bioengineering*. **83** (6), 706, **2003**.
 6. JIAWEI H., JUN L. Aerobic denitrification characteristics of a flow-separation reactor under oxygen-rich environment. *Acta Scientiae Circumstantiae*. **36** (2), 521, **2016**.
 7. HU J., LI J., BIAN W., WANG M. Denitrification characteristics in oxygen-enriched continuous anoxic/aerobic biofilm system for municipal wastewater treatment. *Ciesc Journal*. **65** (10), 4071, **2014**.
 8. PEREIRA A.D., LEAL C.D., DIAS M.F., ETCHEBEHERE C., CHERNICHARO C.A., DE ARAÚJO J.C. Effect of phenol on the nitrogen removal performance and microbial community structure and composition of an anammox reactor. *Bioresource Technology*. **166** (8), 103, **2014**.
 9. WEN Y., WEI C.H. Heterotrophic nitrification and aerobic denitrification bacterium isolated from anaerobic/anoxic/oxic treatment system. *African Journal of Biotechnology*. **10** (36), 6985, **2011**.
 10. CHOU J., BEN-NISSAN B., CHOI A.H., WUHRER R., GREEN D. Conversion of coral sand to calcium phosphate for biomedical application. *J. Aust. Ceram. Soc.* **43** (1), 44, **2007**.
 11. CLESCERI L.S., GREENBERG A.E., EATON A.D. Standard methods for the examination of water and wastewater, 20th ed. APHA, Washington D.C. **1999**.
 12. DELATOLLA R., BERK D., TUFENKJI N. Rapid and reliable quantification of biofilm weight and nitrogen content of biofilm attached to polystyrene beads. *Water Research*. **42** (12), 3082, **2008**.
 13. GAO D.W., WEN Z.D., LI B., LIANG H. Membrane fouling related to microbial community and extracellular polymeric substances at different temperatures. *Bioresource Technology*. **143** (1), 172, **2013**.
 14. HOWARTH R., UNZ R.F., SEVIOUR E.M., SEVIOUR R.J., BLACKALL L.L., PICKUP R.W. Phylogenetic relationships of filamentous sulfur bacteria (*Thiothrix* spp. and *Eikelboom* type 021N bacteria) isolated from wastewater-treatment plants and description of *Thiothrix Eikelboomii* sp. nov. *Thiothrix Unzii* sp. nov. *Thiothrix Fructosivorans* sp. *Int J Syst Bacteriol*. **49** (4), 1817, **1999**.
 15. HUANG X., LI W., ZHANG D., QIN W. Ammonium removal by a novel oligotrophic *Acinetobacter* sp. Y16 capable of heterotrophic nitrification-aerobic denitrification at low temperature. *Bioresource Technology*. **146** (10), 44, **2013**.
 16. LI Y., ZHANG J., CHEN Q., YANG G., CAI S., HE J., ZHOU S., LI S.P. *Dokdonella kunshanensis* sp. nov., isolated from activated sludge, and emended description of the genus *Dokdonella*. *International Journal of Systematic & Evolutionary Microbiology*. **63** (4), 1519, **2013**.
 17. XING W., LI D., LI J., HU Q., DENG S. Nitrate removal and microbial analysis by combined micro-electrolysis and autotrophic denitrification. *Bioresource Technology*. **211**, 240, **2016**.
 18. WANG H., HU C., LI X. Characterization of biofilm bacterial communities and cast iron corrosion in bench-scale reactors with chloraminated drinking water. *Engineering Failure Analysis*. **57**, 423, **2015**.
 19. TIAN H.L., ZHAO J.Y., ZHANG H.Y., CHI C.Q., LI B.A., WU X.L. Bacterial community shift along with the changes in operational conditions in a membrane-aerated biofilm reactor. *Applied Microbiology & Biotechnology*. **99** (7), 3279, **2015**.
 20. Zuber H. Structure of light-harvesting antenna complexes of photosynthetic bacteria and red algae. *Trends in Biochemical Sciences*. **11** (10), 414, **1986**.
 21. CHEN Y., ZHAO Z., PENG Y., LI J., XIAO L., YANG L. Performance of a full-scale modified anaerobic/anoxic/oxic process: High-throughput sequence analysis of its microbial structures and their community functions. *Bioresource Technology*. **220**, 225, **2016**.
 22. KARKMAN A., MATTILA K., TAMMINEN M., VIRTA M. Cold temperature decreases bacterial species richness in nitrogen-removing bioreactors treating inorganic mine waters. *Biotechnology & Bioengineering*. **108** (12), 2876, **2011**.
 23. ARAÚJO A.L.C., OLIVEIRA R.D., MARA D., SILVA S.A. Sulphur and phosphorus transformations in wastewater storage and treatment reservoirs in northeast Brazil. *Water Science & Technology*. **42** (10), 203, **2000**.
 24. ZHAO Y., HUANG J., ZHAO H., YANG H. Microbial community and N removal of aerobic granular sludge at high COD and N loading rates. *Bioresource Technology*. **143**, 439, **2013**.
 25. VANDERMAESEN J., LIEVENS B., SPRINGAEL D. Isolation and identification of culturable bacteria, capable of heterotrophic growth, from rapid sand filters of drinking water treatment plants. *Research in Microbiology*. **168** (6), 594, **2017**.
 26. CHAKRAVARTHY S.S., PANDE S., KAPOOR A., NERURKAR A.S. Comparison of denitrification between *Paracoccus* sp. and *Diaphorobacter* sp. *Applied Biochemistry & Biotechnology*. **165** (1), 260, **2011**.
 27. LIU W., YANG D., CHEN W., GU X. High-throughput sequencing-based microbial characterization of size fractionated biomass in an anoxic anammox reactor for low-strength wastewater at low temperatures. *Bioresource Technology*. **231**, 45, **2017**.
 28. WANG Z., HUANG F., MEI X., WANG Q., SONG H., ZHU C., WU Z. Long-term operation of an mbr in the presence of zinc oxide nanoparticles reveals no significant adverse effects on its performance. *Journal of Membrane Science*. **471**, 258, **2014**.